The Missing Baryon Component: A search for the Cosmic Web using the CMB

Mitchell de Zylva

Supervised by
Dr Chrisitan Reichardt

School of Physics
Faculty of Science
University of Melbourne

October 10, 2019

Submitted in fulfillment of the requirements of the degree of
Master of Science (Physics)

Statement of contribution:

This is to certify that:

- This thesis entitled "The Missing Baryon Component: A search for the Cosmic Web using the CMB" comprises only my original work except where indicated otherwise.
- Due acknowledgement has been made in the text to all other material used.
- The thesis is no longer than 50 pages in length, inclusive of tables, figures, bibliographies and appendices.

.....

Mitchell de Zylva

Acknowledgements:

You put all the people you want to thanks here :)

You need a statement of contribution, which you will sign before you submit.

Abstract

Abstract goes here..

Contents

Chapter 1

Introduction

1.1 The Cosmic Microwave Background

The basis for modern cosmology relies on several fundamental assumptions stemming from observation, the chief of which is the Big Bang Model. Following Hubble's discovery of a relation between distances to galaxies and their recessional velocities, the *Copernican Principle* leads to the conclusion that in the past, objects in the universe were much closer together. His observations gave rise to the Lemaitre's Hubble Law,

$$v \propto d \tag{1.1}$$

This suggests that at some point in the past, the universe was much smaller than it is at present, the conservation of energy then implies that at some point in the past, the universe must have been an incredibly hot, dense environment. Using general relativity, the extrapolation backwards in time yields a singularity of infinite density and temperature, which is commonly called the *Big Bang*

Another assumption stemming from observation is that of isotropy. Based on observation, there appears to be no favoured direction in the universe, since distributions of distant galaxies and other extragalactic sources seem to be evenly distributed across the sky. Perhaps the most spectacular example of this isotropy is the presence of the *Cosmic Microwave Background*.

Discovered in 1964 (**?**), it was noticed that there was isotropic black-body radiation at $T \approx 2.7\,\mathrm{K}$. Since the peak of this radiation is in the microwave section of the electromagnetic spectrum, it was termed the *Cosmic Microwave Background*.

The Cosmic Microwave Background (CMB) provides the most accurate and detailed measures of the primary cosmological parameters to date.

1.2 Cosmological Parameters

For a Λ CDM universe, there are six independant paramters which descirbe the evolution and behaviour of the universe, the physical baryon density $\Omega_b h^2$, the physical dark matter density $\Omega_c h^2$, the age of the universe t_0 (or its reciprocal, the Hubble constant H_0), the scalar spectral index n_s, the curvature fluctuation amplitude Δ^2_R, and the reionisation optical depth τ.

Currently, the highest precision measures of these features from the CMB come from Planck Collaboration et al. (2018), which details that baryonic matter only comprises $\approx 5\%$ of the universe's energy density. In principle, this component of the universe should be directly measurable. At just three minutes after the Big Bang, deuterium can be used as a tracer for this abundance (Steigman, 2007), and at redshift $z \geqslant 2$, the baryon fraction can be found in the absorption lines of quasars

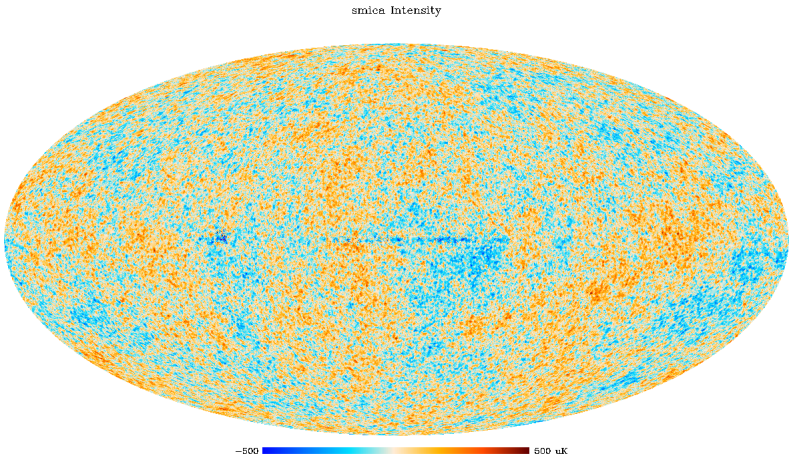

Figure 1.1: *Planck* Satellite Full Sky CMB Map

passing through the diffuse, photo-ionised intergalactic medium, known as the Lyman-α forest (Weinberg et al., 1997). However as the universe evolved, this gas became sparser as it became more ionised. This makes searching for the entirety of the baryon fraction at low redshift difficult. When this fraction is calculated directly from observations, it shows only one tenth of the baryonic content shown in high redshift measurements is contained in galactic structures (Persic & Salucci, 1992). Some revised estimates considered that the limitations of observations were primarily to blame for this discrepency, and not inherent new physics (Bristow & Phillipps, 1994; Fukugita et al., 1998)

The baryon content has been confirmed to a very high accuracy with recent CMB experiments, first with the *Wilkinson Microwave Anisotropy Probe* (WMAP) (Spergel et al., 2007), and then with the *Planck* Satellite (Planck Collaboration et al., 2018). When we quote quantities, we take values from the latest *Planck* paper

Parameter	Value	Error
$\Omega_c h^2$	0.120	±0.001
$\Omega_b h^2$	0.0224	±0.0001
n_s	0.965	±0.004
τ	0.054	±0.007
$100\Theta_\star$	1.0411	±0.0003
H_0 (km s^{-1} Mpc^{-1})	67.4	±0.5

Chapter 2

The Missing Baryon Problem

The Missing Baryon problem is one that arises when we try and make an account of the baryons at low redshift. At high redshift ($z > 2$), the Lyman-α forest provides a good measure of the proportion of baryons, since at these redshifts the majority of the baryons in the universe are contained in diffuse gas. These analyses give a reported value

$$\Omega_{baryon} \geq 0.035$$

Observed light-element ratios and standard nucleosynthesis allows for direct computation of the expected baryon densities, which is in agreement with the above figure (Burles & Tytler, 1998)

$$\Omega_{baryon} = (0.019 \pm 0.001)h^{-2} = 0.039 \pm 0.002$$

The agreement between these two measures of baryon density, and the measurement obtained from the CMB lends confidence to the value obtained.

However, at low redshifts, all analysis indicates that the summing over all observed contributions gives a value of

$$\Omega_{\star} + \Omega_{HI} + \Omega_{H_2} + \Omega_{X-Ray,cl} \approx 0.0068 \leq 0.011$$

This severe discrepency between measurements at high and low redshifts suggests that either the majority of the baryons at low redshifts are yet to be detected, or there are fundamental errors in numerous independant measures of the baryon density at high redshift.

2.1 Stellar Baryons

The most obvious location to search for baryons are in the stellar populations of galaxies. At a broad level, we can imagine that there are two distinct stellar populations which can be considered to be found in high density galaxies; a class of old stars which exists in the spheroidal region of a galaxy, and a class of young stars in the disk region, as well as a third population existing in irregular galaxies.

Estimating the proportion of stellar baryons therfore becomes an exercise in galactic morphology and luminosity density function computation. *** Do I need to go through the explicit calculuation of star densities here?*** Perfoming this calculation gives mean mass density numbers for three classes of stars

$$\begin{aligned}
\Omega_{\text{Spheroid Stars}} &= (0.00180^{+0.00121}_{-0.00085})h^{-1} \\
\Omega_{\text{Disk Stars}} &= (0.00060^{+0.00030}_{-0.00024})h^{-1} \\
\Omega_{\text{Stars in Irregular Galaxies}} &= (0.000048^{+0.000033}_{0.000026})h^{-1}
\end{aligned}$$

These numbers depend on the mass-to-light ratio for age estimation, and so in turn are dependant on the cosmological parameters in a complex way. Even if efforts were made to remove this dependancy by changing the methodology used to calculate the mass-to-light function, the necessity for the new methodology to hold consistent with other measurements would force the dependancy regardless ***(If dynamics were used to estimate M/L, the estimates of)would not depend onh,but in that casehB0.7 would be needed for dynamics toagree with the synthesis calculations. Either way, consis-tency holds forhB0.7 in a low-density universe.)***

2.2 Cold Interstellar Medium

2.3 Lyman α

2.4 OVI and BLA Absorbers

2.5 Hot Gas in Clusters

Chapter 3

The Warm-Hot Interstellar Medium

High resolution hydrodynamical simulations allow us to predict the overall structure of the cold dark matter in the universe (Cen & Ostriker, 1999). These can in turn be used to estimate the baryon distribution at low and moderate redshifts.

It is clear that by the current era, heirachical structure formation collects baryons in gravitational potential wells formed by the dark matter, which moves a significant portion of the baryon component that was previously located in the intergalactic medium at higher redshifts, into structure, such as stars, galaxies, groups, and clusters.

These simulations indicate that the baryons at low redshift fall into four general phases, defined by the overdensity $\delta \equiv \rho/\bar{\rho} - 1$ (where $\bar{\rho}$ is the mean density of baryons).

- Diffuse Gas: $\delta < 1000$, $T < 10^5 K$, Photoionised gas which is visible in Lyman-α absorption spectra
- Condensed: $\delta > 1000$, $T < 10^5 K$, Stars and cool galactic gas
- Hot: $T > 10^7 K$, Galaxy Clusters and Groups
- Warm-Hot: $10^5 K < T < 10^7 K$, Warm-Hot Intergalactic Medium (WHIM)

Simulations (Cen & Ostriker, 1999; Davé et al., 2001) indicate that at redshift $z = 0$ approximately $30 - 40\%$ of baryonic mass is contained within the last catergory, in the WHIM. WHIM gas seems to primarily trace filamentary large scale structures, and clusters around sites of galaxy formation. Because the gas is not bound or virialised, it is apparent that the mechanism which heats it to such high tempratures is shock-heating, caused by gas acreting onto large scale structure. This is consistent with measurements from the soft X-ray background.

Because the temperature and density of the WHIM are correlated, and the WHIM is in turn correlated with the large scale structure, we can use the precense of other tracers of large structure, temperature, and density to search for the baryons contained in the WHIM.

The WHIM is considered to exist in a filamentary web, which has been shock-heated during the process of structure formation to the temperatures described above. It is so highly ionised, and so disperse (with average densities of the order of 10 particles per cubic meter), that they can only emit or absorb far-ultraviolet or soft x-ray photons. These photons are primarily at highly ionised lines of C, O, Ne, and Fe (Cen & Fang, 2006).

Tracking the baryons contained in the WHIM can only be done by exploiting both experimental multiwavelength observations and theoretical calculations. X-Ray and UV spectroscopic surveys

measure the mass of WHIM using the relative and absolute metal content, and the ionisation correction. These can be then combined with optical and infrared photometry and spectroscopy which measure dark matter concentrations by measuring galaxy density around WHIM filaments. These observations then feed into simulations, which allow for more detailed study of virialised structure and the intergalactic medium.

The intensity of the signals obtained from direct observation is low in both the UV and the X-Ray bands, both as a result of the density and the relatively small size of the filaments (1 - 10 Mpc). Direct detection ideally requires large field of view and effective area imager-spectrometers, which is not currently available. The strategy that can best be utilised with current technology involves searching for discrete absorption lines in the spectra of bright, featureless background astrophysical sources.

The key feature necessary to detect an absorption line is the ratio between the line wavelength and its equivalent width, called its transition contrast. For the dominant absorption lines of oxygen, in this case OVI, the current resolving power of UV spectrometers is sufficient to measure its transition contrast, but for the X-Ray band, it is worse, and so searches for the WHIM have proven more fruitful in the UV band than in the X-Ray (Danforth & Shull, 2005; Richter et al., 2006). Using hydrodynamical simulations to replicate the observed absorption per unit redshift, it can be shown that if the WHIM was based solely on the OVI absorption, it would only account for approximately 10 percent of the missing baryon component.

An alternative method for searching for the missing mass is to look for hydrogen absorption in broad Ly-α absorbers (BLAs). At the temperatures that the WHIM is thought to exist at, most of the hydrogen will be ionised, but left-over neutral hydrogen can still imprint Lyman series absorption onto the ultraviolet spectra of background objects. These lines will be be very broad, given that the temperatures of the WHIM create a Doppler parameter of the order of $b \approx 40\,\mathrm{km/sec}$. This technique again gives a similar measurement to that done with OVI absorbers, and so suggests that BLAs and OVI absorbers can be considered to be good tracers of the WHIM, but aren't sufficient to probe the entirety of the missing mass due to the majority of it existing in temperatures only probed by the X-Ray band.

Comprehensive studies of the WHIM therefore require both the UV and X-Ray bands, since the X-Ray is crucial to detect the WHIM, and provide an accurate ionisation correction, and the UV is necessary to measure the assosciated amount of HI and hence the baryonic mass of the system.

According to theory, the chances of finding a WHIM filament along an arbitrary line of sight increases with the path length crossed between the observer and the beacon used to obtain the X-Ray images of intervening space, and the inverse of the baryon column density in the filament in question. This tells us that the larger the amount of baryons in the filament, the lower the probability of finding one. It can be shown that the detection of the WHIM is within the range of instrumentation currently, but it requires long observation times, making it untenable. Searching for an alternative tracer for the WHIM is therefore necessary to accurately locate the missing baryon content.

Chapter 4

The Sunayev-Zeldovich Effect

*** NEED SOURCES FOR ATOMIC PHYSICS OF Sunyaev-Zel'dovich effect ***

4.1 Atomic Physics

The thermal Sunyaev-Zel'dovich effect is one possible tracer. Sunyaev-Zel'dovich effect refers to the inverse compton scattering of CMB photons off of hot electrons in the WHIM.

Compton Scattering is a form of inelastic scattering between light and free charged particles, such as electrons. There is a momentum transfer between the photon in the interaction, and the charged particle, and so the photon's wavelength changes as a result of the scattering.

It was first described in the context of X-rays interacting with electrons in atoms, and so regular Compton Scattering is taken to describe the interaction between a high energy photon, and a low energy particle (or one at rest). By applying principles of conservation of momentum, and conservation of energy, the formula for the shift in wavelength as a result of this scattering is given by

$$\Delta\lambda = \frac{h}{m_e c}\left(1 - \cos\theta\right) \tag{4.1}$$

where m_e is the mass of the electron, and θ is the angle between the incident and scattered trajectories.

For the Sunyaev-Zel'dovich effect however, the energies of the photons in question are much lower than the energies of the electrons involved, so the frequency shift is parametrised by something called the Compton y-parameter. The full expression for the Compton y-parameter is

$$y = \int \frac{k_B T_e}{m_e c^2} n_e \sigma_T d \tag{4.2}$$

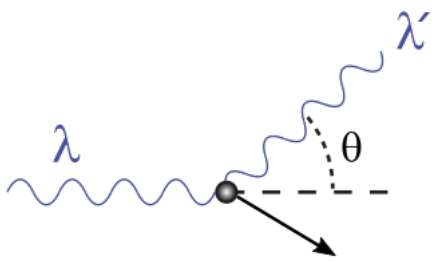

Figure 4.1: Compton Scattering

where $m_e c^2$, k_B, and σ_T are the electron rest mass energy, Boltzmann constant, and Thompson Cross Section respectively. These are all well defined constants, and so have no effect on the integration. The y-parameter therefore amounts to the line-of-sight integration over $n_e T_e$, which are the electron gas density and temperature. The degeneracy between temperature and pressure can be broken in principle by obtaining measurements of one of the two quanties, which we in princple take from hydrodynamical simulations.

4.2 CMB Signal

Given the signal-to-noise ratio expected for the thermal Sunyaev-Zel'dovich effect of a single filament, many such filaments must be co-added, so as to drive the signal-to-noise to a detectable level. Initially outlined in Clampitt et al. (2016) for application to weak gravitational lensing maps, it was found that stacking $\tilde{1}35\ 000$ pairs yielded a filament mass at $\tilde{4}.5\ \sigma$ confidence. Further follow up using the Canada France Hawaii Telescope Lensing Survey (CFHTLenS), and the Sloan Digital Sky Survey's (SDSS) Luminous Red Galaxy (LRG) catalogue by Epps & Hudson (2017) detected the weak lensing signal from stacked filaments at 5σ confidence.

Investigations by Van Waerbeke et al. (2014), Ma et al. (2015), and Hojjati et al. (2015) established firmly that there is a correlation between weak gravitational lensing from CFHTLenS and tSZ signals from *Planck*, which suggests that we can use tSZ in the same way as weak lensing, without having to be careful about the peculiarities assosciated with weak lensing, such as sufficiently nulling spherical components. This was further reinforced by Hill & Spergel (2014), who reported a 6.2σ correlation between the *Planck*lensing potential and the *Planck*tSZ map.

Chapter 5

Stacking Methodology

Initially outlined in Clampitt et al. (2016), the stacking algorithm involves creating a list of galaxy pairs, which we would expect to see a filament between, and then using those pairs, forming a normalised two-dimensional image, with the galaxies of the pair being placed on two points in the image, and stacking them until the signal to noise is sufficient to be measurable.

The intial problem faced involves generating the galaxy pairs from the Dark Energy Survey redMaGiC Catalogue. The Year 1 Catalogue consists of 0.65 million red-sequence galaxies in the redshift range $0.15 < z < 0.9$. The algorithm used by the Dark Energy Survey to select these red-sequence galaxies provides redshift estimates of very high quality and very low bias ($\lesssim 0.5$ percent). They also have very low scatter, and a very low rate of catastrophic outliers. The algorithm yields superior photo-z performance than the colour-cut methodology used to definte the Sloan Digital Sky Survey CMASS catalogue (Rozo et al., 2016).

Pairs were generated by making use of kD-trees. A generalisation of a binary tree, the kD tree is one where every leaf node is representative of a k dimensional point. Each non-leaf node is one that 'splits' the space into two parts, whereby points to the left of this hyperplane are represented by the left sub-tree, and to the right are represented by the right sub-tree. When we apply this to our galaxy catalogue, we first locate them in 3 dimensional space, by converting their RA, Dec, and redshift into a comoving 3D coordinate. They are then placed in a kD tree, and any pair which has a radial comoving separation of less that $10h^{-1}$ Mpc, and transverse comoving separation range of $6 - 14h^{-1}$ Mpc is considered to have a filament (Clampitt et al., 2016).

From this, approximately 340,000 galaxy pairs were constructed with a mean angular separation of ~ 31.6 arcmins, and a mean comoving separation of $11.9h^{-1}$ Mpc.

Functionally, this means that the pair is located in the CMB, and a cutout of the CMB is taken around them. They are then rotated, so they are all aligned along the same axis. This subsequent image is then rescaled, so that each pair is located at the same point in the image. They are then added together.

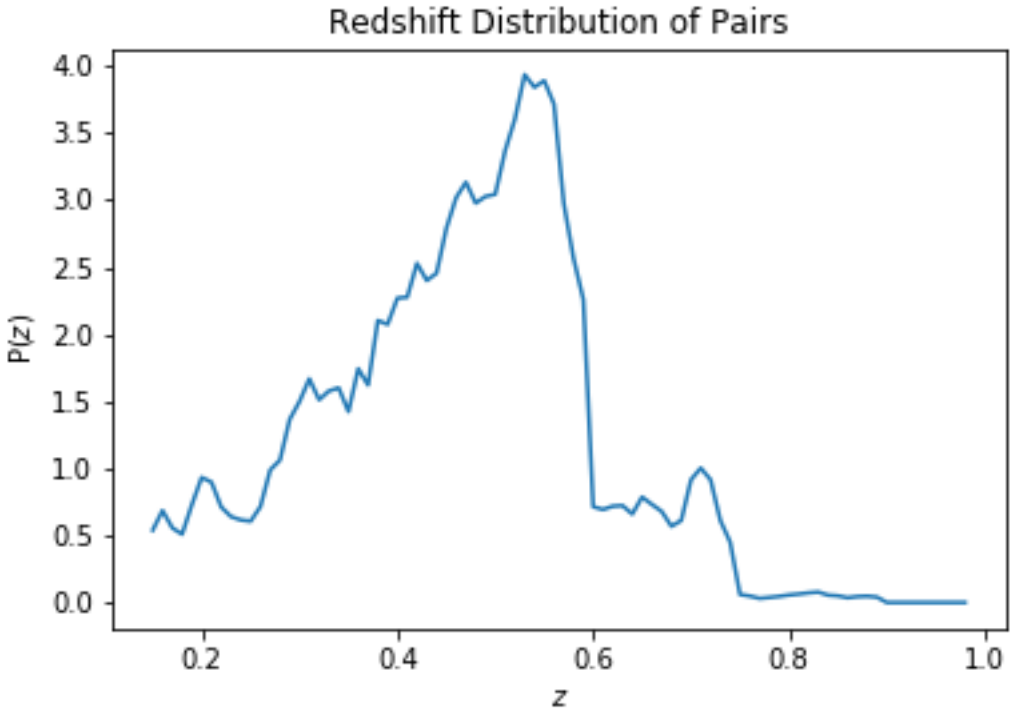

Figure 5.1: Redshift Distribution of Galaxy Pairs

Chapter 6

Results

This is another example chapter. I imagine this would be one of the last chapters...

> This line is indented

This line isn't
Nor is this one cos it's right below another line.

Here's a reference: **?**
Here's a reference in brackets: (**?**)

Chapter 7

Conclusion

All your Concluding.

Bibliography

Bristow, P. D. & Phillipps, S., 1994, On the Baryon Content of the Universe, *MNRAS* 267, 13

Burles, S. & Tytler, D., 1998, Measurements of the deuterium abundance in quasar absorption systems, in Mezzacappa, A., editor, *Stellar Evolution, Stellar Explosions and Galactic Chemical Evolution*, p. 113

Cen, R. & Fang, T., 2006, Where Are the Baryons? III. Nonequilibrium Effects and Observables, *ApJ* 650, 2, 573

Cen, R. & Ostriker, J. P., 1999, Where Are the Baryons?, *ApJ* 514, 1, 1

Clampitt, J.; Miyatake, H.; Jain, B. & Takada, M., 2016, Detection of stacked filament lensing between SDSS luminous red galaxies, *MNRAS* 457, 3, 2391

Danforth, C. W. & Shull, J. M., 2005, The Low-z Intergalactic Medium. I. O VI Baryon Census, *ApJ* 624, 2, 555

Davé, R.; Cen, R.; Ostriker, J. P.; Bryan, G. L.; Hernquist, L.; Katz, N.; Weinberg, D. H.; Norman, M. L. & O'Shea, B., 2001, Baryons in the Warm-Hot Intergalactic Medium, *ApJ* 552, 2, 473

Epps, S. D. & Hudson, M. J., 2017, The Weak Lensing Masses of Filaments between Luminous Red Galaxies, *MNRAS* 468, 3, 2605

Fukugita, M.; Hogan, C. J. & Peebles, P. J. E., 1998, The Cosmic Baryon Budget, *ApJ* 503, 2, 518

Hill, J. C. & Spergel, D. N., 2014, Detection of thermal SZ-CMB lensing cross-correlation in Planck nominal mission data, *J. Cosmology Astropart. Phys.* 2014, 2, 030

Hojjati, A.; McCarthy, I. G.; Harnois-Deraps, J.; Ma, Y.-Z.; Van Waerbeke, L.; Hinshaw, G. & Le Brun, A. M. C., 2015, Dissecting the thermal Sunyaev-Zeldovich-gravitational lensing cross-correlation with hydrodynamical simulations, *J. Cosmology Astropart. Phys.* 2015, 10, 047

Ma, Y.-Z.; Van Waerbeke, L.; Hinshaw, G.; Hojjati, A.; Scott, D. & Zuntz, J., 2015, Probing the diffuse baryon distribution with the lensing-tSZ cross-correlation, *J. Cosmology Astropart. Phys.* 2015, 9, 046

Persic, M. & Salucci, P., 1992, The baryon content of the universe, *MNRAS* 258, 1, 14P

Planck Collaboration; Aghanim, N.; Akrami, Y.; Ashdown, M.; Aumont, J.; Baccigalupi, C.; Ballardini, M.; Banday, A. J.; Barreiro, R. B. & Bartolo, N., 2018, Planck 2018 results. VI. Cosmological parameters, *arXiv e-prints* arXiv:1807.06209

Richter, P.; Savage, B. D.; Sembach, K. R. & Tripp, T. M., 2006, Tracing baryons in the warm-hot intergalactic medium with broad Ly α absorption, *A&A* 445, 3, 827

Rozo, E.; Rykoff, E. S.; Abate, A.; Bonnett, C.; Crocce, M.; Davis, C.; Hoyle, B.; Leistedt, B.; Peiris, H. V.; Wechsler, R. H. et al., 2016, redMaGiC: selecting luminous red galaxies from the DES Science Verification data, *MNRAS* 461, 2, 1431

Spergel, D. N.; Bean, R.; Doré, O.; Nolta, M. R.; Bennett, C. L.; Dunkley, J.; Hinshaw, G.; Jarosik, N.; Komatsu, E.; Page, L. et al., 2007, Three-Year Wilkinson Microwave Anisotropy Probe (WMAP) Observations: Implications for Cosmology, *ApJS* 170, 2, 377

Steigman, G., 2007, Primordial Nucleosynthesis in the Precision Cosmology Era, *Annual Review of Nu-*

clear and Particle Science 57, 1, 463

Van Waerbeke, L.; Hinshaw, G. & Murray, N., 2014, Detection of warm and diffuse baryons in large scale structure from the cross correlation of gravitational lensing and the thermal Sunyaev-Zeldovich effect, *Phys. Rev. D* 89, 2, 023508

Weinberg, D. H.; Miralda-Escudé, J.; Hernquist, L. & Katz, N., 1997, A Lower Bound on the Cosmic Baryon Density, *ApJ* 490, 2, 564